Modeling of microkinetics in heterogeneous catalysis by means of frequency response techniques

Abdul R. Garayhi, Frerich J. Keil*

Chair of Chemical Reaction Engineering, Technical University of Hamburg-Harburg, Eissendorfer Str. 38, D-21073 Hamburg, Germany

Abstract

A frequency response (FR) technique for the instationary determination of kinetic constants is presented. Reliable quantitative information is obtainable for the description of non-stationary reactor operation. Two models for the evaluation of kinetic FR experiments are described, an analytical expression for a quick parameter determination and a rigorous approach for the determination of a microkinetic expression. The model will be employed for the evaluation of experiments. As an example, the combustion of methane on a supported palladium catalyst will be investigated. © 2001 Elsevier Science B.V. All rights reserved.

Keywords: Temporal analysis of products; Microkinetics; Heterogeneous catalysis; Frequency response; Combustion

1. Introduction

The steady-state behavior of many chemical processes was optimized for decades. Meanwhile the transient behavior is also a subject of interest for two different reasons. First, the overall economics of a plant can in many cases be improved by a non-stationary operation. Plants that are usually run under steady state conditions are sometimes also operated dynamically, e.g. start-up, shut-down, or switching between different stationary states if the feed or product specifications are varied or the load is changed. Product losses and switching times are to be minimized in these cases. The yield per unit volume and time has been improved significantly in some examples. Secondly, for a modern safety analysis, it is required not only to describe the steady-state operation but also the behavior during faults reliably.

There are more essential parameters for the description of a reactor under dynamic operation than under steady state. Not only steady-state reaction rate constants, adsorption constants, and pore effectiveness factors, but also dynamic constants like adsorption capacities, diffusional penetration depths, and surface restructuration times are required. This inevitably requires non-stationary measurements under reacting conditions. The quantities for the description of the thermal behavior like heats of reaction, thermal conductiv-

ities and diffusivities may also be found from steady-state or non-reacting experiments. Therefore, the determination of these parameters is not described here. Muralidhar and Mishra [1] present a frequency response (FR) method for the determination of axial and radial heat dispersion coefficients.

Experiments under dynamic conditions can also give important insight into the reaction mechanism. For a correct description of the steady state, a detailed knowledge of the reaction mechanism is desirable. While it is usually easy to find the overall reaction kinetics if the mechanism and the kinetic expression of the elementary steps are known, it is at present impossible to solve the inverse problem in a common case. This would be required if the kinetic expressions of the elementary steps are to be obtained from the overall kinetic behavior. Asadullin [2] gives an example where at least the number of solutions may be found in a special case. With the present mathematical tools, it seems to be impossible to determine the reaction mechanism and the intermediate species on the catalyst surface from the gas composition in the bulk phase of the reactor. This dilemma can be avoided in two ways. In the first approach, reaction intermediates are determined to reveal as much of the mechanism as possible. Such measurements usually require specialized laboratory devices (e.g. temporal analysis of products (TAP) reactor, in situ spectroscopy techniques [3]). The operating conditions of these laboratory reactions are often far away from the operating conditions of technical production plants (temperature/pressure gap). Additionally, the catalyst samples are often prepared in a special manner (e.g. single crystals) and they are significantly different

---

* Corresponding author. Tel.: +49-40-7718-3042;
fax: +49-40-7718-2145.
E-mail address: keil@tu-harburg.de (F.J. Keil).

Nomenclature

a	Fourier coefficient
$\tilde{a}$	experimental Fourier coefficient
A	relative amplitude
A_0	frequency factor
b	volume specific surface area
Bi	Biot number
c	concentration
c_p	specific heat
D	diffusivity
$\boldsymbol{e}$	vector, all elements 1
E_0	activation energy
h	specific enthalpy
k	mass transfer coefficient
K_0	initial asymptote
K	Langmuir adsorption constant
L	characteristic length (e.g. pellet diameter)
n	number of moles
n_c	number of components
$\boldsymbol{n_R}$	number of reactions, number of moles
$\dot{n}$	molar flux
p	pressure
r	radius
r_R	reaction rate
R	universal gas constant
t, t_r	time, residence time
T	temperature
T_E	time constant
V	volume
$\tilde{V}$	superficial volume
x	mole fraction
z	dimensionless spatial coordinate
$\tilde{z}$	spatial coordinate, here pellet radius

Greek symbols

α	heat transfer coefficient
β^0	viscous factor
δ	dimensionless diffusivity
Δ	characteristic diffusivity
ε	porosity
η	viscosity
φ	phase lag
κ	linear adsorption constant
κ_{dim}	dimensionless specific surface area
κ_R	heterogeneous reaction constant
λ	thermal conductivity
θ	dimensionless time, coverage
ρ	density
τ	tortuosity
τ_a	apparent residence time
υ	stoichiometric coefficient
ω	dimensionless reaction rate
ψ	pressure ratio

Superscripts and subscripts

c	component
gas	gas phase
i	number of component
in	feed
P	pore
R	reactor bulk phase, reaction
solid	adsorbed phase, adsorbed phase plus pellet
s	surface

from the catalysts used in technical reactors (material gap). So, it is not ensured that the mechanism found by these methods will also be applicable for production conditions.

The second approach is to approximate the real mechanism by idealized model mechanisms. This approach is very successfully established for the description of the steady-state behavior. Many reactions may be described by the well-known Langmuir–Hinshelwood–Hougen–Watson scheme, although the mechanistic assumptions for these expressions are only valid in exceptional cases. Boudart has called this the "paradox of surface catalysis" [4]. Nevertheless, Kiperman et al. [5] have listed many examples where an inhomogeneous modeling of the surface active sites is absolutely required for a sufficiently reliable description of the reactions, and where the common model mechanisms are not applicable.

Instationary experiments were reviewed by several authors (see for example [6–23]). Methods of microkinetic measurements and modeling were compiled by Dumesic et al. [24]. There is a close interrelation between experiments and microkinetic modeling [18,25]. Stoltze [26] reviewed microkinetic simulation approaches.

In the present paper a FR method (sinusoidal stimulation) for the determination of kinetic constants, and, to a certain extent, of reaction mechanisms is presented. Furthermore, the stimulating frequency is varied, and the response is determined. Although the FR techniques are in widespread use for the measurement of diffusion coefficient and sorption in zeolites and mass transfer kinetics on catalytic surfaces, only a very few applications of this method to heterogeneous catalysis under reactive conditions with the aim of finding microkinetic reaction rate constants were published yet [27–43]. Yasuda [44] reviewed FR methods. In all the papers on FR methods in catalysis published previously either the pressure at the inlet of a packed bed, Δp_{in}, was varied sinusoidally in a flow system and the response was obtained from the data of Δp_{out} at the exit, or the gas space of a batch system was varied sinusoidally and the response was obtained from Δp in the chamber.

The goals of the present investigations are as follows.

- A model will be developed that allows a reliable description of the reaction kinetics under instationary conditions. The multicomponent diffusion within the pellet is taken into account.

- The kinetic expression includes the dynamics on the catalyst surface.
- An experiment is described which allows to determine the concentration of active sites on the catalyst under reactive conditions. A discrimination between different kinetic expressions is possible.
- The methane combustion is investigated.

2. Method

As steady-state investigations of the reactor behavior cannot reveal the transient behavior reliably, it is unavoidably necessary to conduct experiments under transient conditions. Different input signals are suggested in the literature. These can be divided into methods with varying residence time, temperature, feed composition, or a combination of these parameters.

A change in the composition shows the clearest deviation of the steady state from the non-steady state catalyst behavior and will for this reason be employed in the present work. In many works step or square waves signals are used (see for example [45]). In such experiments, the system is excited on all frequencies. These signals, which are advantageous for the investigation of many linear systems, are not advantageous for the quantitative investigation of non-linear chemical systems. In case of non-linear systems — as in the present subject due to the chemical interaction — it is impossible to infer from the output frequency to the exciting frequency by simple means. Except for linear systems, this leads to a high uncertainty of quantitative results. Linear systems do not cause such problems. Quantitative information can be obtained especially by a multi-frequency excitation [46]. By definition, their output signal can be regarded as the combination of the output signal of the exciting frequencies. A frequency portion of the output signal is the response to the same frequency portion in the input signal. A considerable part of the FR is the obtainable from one step experiment by Fourier transform.

As chemical reactors without reaction may be regarded as linear systems, such multi-frequency excitations are perfectly suitable for qualitative investigations, since no important frequency is omitted. Examples for successful mechanism elucidations are numerous. However, the FR cannot be found from the step response as the system frequency may be different from the exciting frequency. The evaluation is also restricted to relatively slow processes as Shannon's theorem restricts the information obtainable from discrete measurements. In single-frequency periodic experiments, it is possible to determine the FR by the method presented here as the expected frequency of the system response is known. Additionally, the step response is highly dominated by fast processes, e.g. intraparticle diffusion or fast adsorption, whereas the slower processes are also important for investigation. Simulations also indicate that step signal experiments are not suitable for obtaining quantitative results,

since they are very sensitive to small perturbations. For the quantitative evaluation in the present work, unifrequent input signals are required, i.e. a sinusoidal change at the inlet composition at a fixed feed temperature and space velocity. Comparable measurements were already successfully made for the determination of reactor properties [27] and adsorption constants [47]. A periodic operation may also eliminate the effects due to an activity change, which leads to a clear overshoot response in a step response experiment. Such a case is given in the present work. An advantage of the periodic measurements is to obtain the active capacity and thus the turnover frequency of a catalyst under reaction conditions independently from the adsorption sites.

3. Theory

Different reactors are well-known for laboratory-scale experiments. Differential reactors, which only give a small conversion while the reaction mixture passes the fixed-bed, are preferred for the investigation of heterogeneously catalyzed reactions, because many properties of state can be measured easily. Differential reactors are usually designed as recycle reactors with external or internal recycle to show the hydrodynamic and kinetic behavior of an ideal CSTR. In contrast, long fixed-beds have the disadvantage that the temperature and concentrations are spatially inhomogeneous. Such equipment offers the advantage that the operation may be more similar to production plants, so a scale-up is easier and more reliable. If the real hydrodynamic behavior is to be taken into account in the parameter evaluation, cell or dispersion models may be employed. Cell models extend the description of idealized CSTRs to the description of real reactors. Reactors are modeled as a series of tanks that are coupled by the reaction mixture streams. For a single phase reaction, only forward streams of a one-dimensional series are required for a proper description. Multi-dimensional models and recycle streams are used for a complex geometry or multiphase reactors. On the other hand, dispersion models extend the concept of a tube reactor to the description of real reactors with backmixing. Deviation from plug-flow behavior is given by one or more parameters, the dispersion coefficients.

Feeding the reactants into a CSTR with sinusoidally varying inlet composition will result in a periodic composition profile at the outlet. The oscillations are sinusoidal in the case of a linear (e.g. inert) system. Under reacting conditions the system is usually non-linear and the output signal is no longer harmonic. For a mathematical description of such a reactor and, therefore, for the parameter estimation, there are mainly two possibilities: on the one hand a linearized solution, on the other hand a numerical integration of the describing differential equation. Both methods are presented here, because the evaluation of the linearized equations is a method easy to apply for the description of the transient operation. But as the reaction leads to a highly non-linear

behavior, a detailed simulation is usually required. In the subsequent sections a hierarchy of models of increasing sophistication will be presented.

3.1. Linearized model

For a linear description of a reaction system some assumptions are made as follows.

- One reactant is supplied to the reactor in such excess that the variation in concentration is negligible.
- The system is isothermal. As the temperature dependency of the reaction is usually non-linear (e.g. Arrhenius expression) this assumption is essential to a linear model.
- The volumetric flow is constant and not affected by reaction or sorption.
- Mass transfer resistance can be included into the kinetic expression by constant effectiveness factors.

The reactant A is supplied with a harmonically oscillating concentration. The concentration in the reactor will also oscillate harmonically.

Since the concentrations in the reactor are spatially homogeneous, the reaction is assumed to take place in the entire volume $\widetilde{V}$. The material balance is

$$\frac{dn_A}{dt} = \dot{n}_{in} - \dot{n}_{out} + \nu_A r_R \widetilde{V} \tag{1}$$

where $\widetilde{V}$ is a volume for describing the reaction rate, it may be different from the physical reactor volume V if sorption effects become important. The total number of moles consists of the amount adsorbed on the catalyst and the amount in the bulk gas. If the ideal gas law is valid, the number of moles may be calculated according to

$$n_A = \frac{p_A}{RT}(V_{gas} + V_{solid}\kappa) \tag{2}$$

where $\kappa = (n_{A,ads}RT)/(V_{solid}p_A)$ is the linear adsorption constant. So the material balance (1) becomes

$$\frac{dp_A}{dt}\frac{1}{RT}(V_{gas} + V_{solid}\kappa) = \dot{V}_0 c_0(t) - \dot{V}_0 c(t) + \nu_A r_R \widetilde{V} \tag{3}$$

If the apparent residence time

$$\tau_a = \frac{V_{gas} + V_{solid}\kappa}{\dot{V}_0} \tag{4}$$

and the heterogeneous reaction rate constant

$$\kappa_R = \frac{\kappa \widetilde{V} k_R}{V_{gas} + V_{solid}\kappa} \tag{5}$$

are introduced, the reaction system is described by the differential equation

$$c_A(t) + \frac{dc_A}{dt}\frac{1}{(1/\tau_a) + \kappa_R} = \frac{1/\tau_a}{(1/\tau_a) + \kappa_R}c_{A,in}(t) \tag{6}$$

The FR of this system is given by the relative amplitude

$$A(T) = \frac{K_0}{\sqrt{1 + (T_E/T)^2}} \tag{7}$$

and the phase lag

$$\varphi(T) = -\arctan\frac{T_E}{T} \tag{8}$$

with the initial asymptote

$$K_0 = \frac{1/\tau_a}{(1/\tau_a) + \kappa_R} \tag{9}$$

and the time constant

$$T_E = \frac{1}{(1/\tau_a) + \kappa_R} \tag{10}$$

As the relative amplitude may be obtained with higher precision in adsorption experiments [29], the phase lag is not used for the evaluation in the present work. However, the phase lag gives valuable information on the experimental conditions. A deviation from the theoretical phase lag indicates dead volumes in the set-up. Other dead times may occur due to an improper experimental set-up, e.g. a fixed-bed in a differential reactor, i.e. such long that a large gradient concentrations may occur if fast processes are kinetically limited. As a consequence the conversion along the bed is no longer of differential type.

The FR experiments give κ_R and τ_a, which can also be treated as independent parameters when used for the description of the reaction. The values κ_R and τ_a may be obtained either by a numerical fit of Eq. (7) to the experimental data or by a graphical method from an asymptotic approximation in the Bode diagram [48].

The amplitudes of the input and output signals are obtained from the measured concentration profiles graphically or by Fourier transformation.

3.2. Simplified non-linear model

A more detailed description of the reactor is possible, if the temperature and concentration profiles are determined numerically. At first, a homogeneous model with two phases, a gaseous and an adsorbed phase, is employed in the present example. A heterogeneous model is described below. Such a heterogeneous model is useful only, if the transport within the catalyst pellets has an important influence on the total behavior of the reaction system.

The following assumptions are made for the homogeneous model.

- The phases are homogeneously dispersed in the whole reactor: a solid phase with adsorbed species and a gaseous phase.
- There are no spatial gradients of temperature, pressure, and composition (CSTR).

- Thermal effects are neglected here, as a comparability to the linear method is strived for. It is easy to find the necessary equations (e.g. by Arrhenius factors) for all reactions to include thermal effects. However, the expressions must be selected carefully, for reasonable results, theoretical information should be included.
- Chemical reactions may take place between species of the adsorbed and the gaseous phase or between species within each phase.
- Adsorption/desorption processes are regarded as chemical reactions. They are treated as being kinetically limited. An equilibrium approach may be included (according to the rate at which the variables of state in the reactor change, the external and internal diffusion processes become rate determining. In these cases the present assumption might not be valid and a more elaborate model like the one presented below is essential).
- For a simplified investigation, the reaction mechanism is restricted to a Langmuir–Hinshelwood type or an Eley–Rideal type here. In reality these mechanisms are distorted due to surface inhomogenities, intermediate reactions, interactions between adsorbed species, etc. Since the vast majority of the catalytic processes can be described by kinetic expressions that were derived for these mechanisms in the steady state, the further investigation is limited to these cases in the present work. However, the experimental method and the evaluation method are not restricted to these model mechanisms.

Even in the non-stationary state — as in the steady state — caution is necessary to use kinetic information as a hint to the underlying mechanism, but sometimes characteristic qualitative phenomena occur, that will exclude some mechanisms. Such phenomena are an overshoot response to a step change in the input signal which may indicate a change in the catalyst activity, e.g. due to restructuration, a change in the oxidation state or adsorption/desorption phenomena. An improved average conversion in periodic operation compared to a steady-state operation may occur in the case of a competitive adsorption.

3.3. Model equations

From the material balances in a CSTR, a system of ordinary differential equation (ODE) can be found for the gaseous and the adsorbed species.

$$\frac{dc_{gas}}{dt} = \left(c_{in}(t) - \left(1 + \varepsilon(1-\varepsilon)\frac{t_r}{c_0} e^T \upsilon_{gas} r_R \right) c(t) \right) \frac{1}{t_r \varepsilon}$$
$$+ (1-\varepsilon)\upsilon_{gas} r_R \tag{11}$$

$$\frac{dc_{ads}}{dt} = \varepsilon \upsilon_{solid} r_R \tag{12}$$

The rates of reaction have to be corrected to the volume of the phases by the factors ε and $(1-\varepsilon)$, because reactions between species of both phases may occur (e.g. Eley–Rideal

type reaction or sorption processes), and the same kinetic expression is to be employed for both phases. The disadvantage is that the kinetic expression is no longer independent of the model equations. This disadvantage cannot be avoided in a two-phase model.

The concentration of adsorbed species

$$c_{i,ads} = \frac{n_{i,ads}}{V_{solid}} \tag{13}$$

is related to the volume of the support including the adsorbed phase, not to the surface area, for a common formulation, but it may easy be adopted to a surface kinetics in any special case.

For the determination of the kinetic constants, the ODE system is numerically integrated and a Fourier transformation of the concentration profiles in the time domain is carried out. The kinetic parameters are afterwards determined by minimization of the objective function

$$F(k) = \sum_{i=1}^{n} \sum_{j=0}^{l} (a_{j,n} - \widetilde{a}_{j,n})^2 \tag{14}$$

with $\widetilde{a}$ the Fourier coefficients that were experimentally obtained.

In the time domain the profiles are affected by experimental errors. For the present calculations, only the zeroth and the first coefficient are employed for the fitting procedure, so the Fourier transformation gives a mean behavior. The zeroth Fourier coefficients are twice the mean concentration of each component, the first Fourier coefficients are the amplitudes of the best approximating sine function (least squares minimum). Higher coefficients are an indicator to the non-linearity of the system equations.

4. Rigorous non-linear model

In order to check the reliability of the parameters a more elaborate model was developed, since mass transfer is always limiting at the beginning of certain transient processes (e.g. switch-on of the feed mixture) [49] and mass-transfer limitations may occur in unsteady-states operation, even if the effectiveness factor is close to unity in the steady state.

The concentration profiles inside the catalyst particles are taken into account, so that no assumptions on the effectiveness factors are required. The catalyst properties like distribution of the active sites or the transport properties (pore radius or permeability) may also be inhomogeneous. Such rigorous models are unavoidably necessary if catalyst restructurations are of great importance and the effects are to be investigated.

Some assumptions are made in addition to those in the homogeneous model.

- The reactor is described by a cell model. Other reactor models like one-, two-, or three-dimensional dispersion

models may be employed. The hydrodynamics of the reactor has to be known in such cases. The main reason for choosing a cell model in the present example is the computational effort. Details of the cell model can be seen from Section 3.

- Three regions are distinguished in each cell: the outer gas phase in the reactor, the gas inside the pellets and the adsorbed phase on the catalyst surface.
- The gas transport within the pores is described by the dusty-gas model [50].
- Mass transfer resistance by the outer boundary layer may be included.

The equations below are valid for slabs (e.g. for modeling a monolith catalyst) for cylinders with sealed top and bottom ends (which are frequently used in catalytic experiments) or for spheres (many catalysts that are made by granulation) if Cartesian, cylindrical, or spherical coordinates are employed. If it is not stated otherwise, spherical coordinates apply in the present paper. Note that the equations in the present notation are not applicable for the description of spheres in Cartesian coordinates. One should keep in mind that one-dimensional models are employed (radius of a sphere or cylinder, thickness of a slab).

The material balance within the radially symmetric catalyst pellet leads to the system of partial differential equations (PDE).

$$
\frac{\partial c}{\partial t} = \frac{\partial}{\partial \widetilde{z}} \left(cRT \frac{r_P^2}{8\eta} \frac{\varepsilon}{\tau} \frac{\partial c_t}{\partial \widetilde{z}} + \boldsymbol{D} \frac{\partial c}{\partial \widetilde{z}} \frac{\varepsilon}{\tau} + \frac{1-\varepsilon}{\tau} \boldsymbol{D}^S \frac{\partial c}{\partial \widetilde{z}} \frac{\varepsilon}{\tau} \right)
$$
$$
+ \sum_j^{n_R} \nu_j r_j \tag{15}
$$

The temperature profile within the particle is given by the PDE system

$$
\frac{\partial T_{\text{solid}}}{\partial t} (1-\varepsilon) \rho c_{\text{p,solid}} \boldsymbol{e}^T c_{\text{solid}} = \frac{1-\varepsilon}{\tau} \frac{\partial}{\partial \widetilde{z}} \left(\lambda \frac{\partial T_{\text{solid}}}{\partial \widetilde{z}} \right)
$$
$$
+ \sum_j^{n_R} H_{R_j} r_j (1-\varepsilon) + \alpha a (T_{\text{gas}} - T_{\text{solid}}) + \sum_i^{n_c} h_i(\widetilde{z}) \frac{\partial c_i}{\partial t} (1-\varepsilon)
$$
$$
+ \sum_i^{n_c} \frac{1-\varepsilon}{\tau} \left[\boldsymbol{e}_i^T D^S \frac{\partial c_i}{\partial \widetilde{z}} \right] c_{\text{p},i} \frac{\partial T_{\text{solid}}}{\partial \widetilde{z}} \tag{16}
$$

and

$$
\frac{\partial T_{\text{gas}}}{\partial t} \varepsilon c_{\text{p,gas}} \boldsymbol{e}^T c_{\text{gas}} = \frac{\varepsilon}{\tau} \frac{\partial}{\partial \widetilde{z}} \left(\lambda \frac{\partial T_{\text{gas}}}{\partial \widetilde{z}} \right) - \sum_j^{n_R} H_R r_j \varepsilon
$$
$$
+ \alpha a (T_{\text{solid}} - T_{\text{gas}}) + \sum_i^{n_c} h_i(\widetilde{z}) \frac{\partial c_i}{\partial t} \varepsilon + \sum_i^{n_c} \frac{\varepsilon}{\tau} \frac{\partial}{\partial \widetilde{z}} \boldsymbol{e}^T
$$
$$
\times \left(c_{\text{gas}} RT \frac{r_P^2}{8\eta} \boldsymbol{e}^T \frac{dc_{\text{gas}}}{d\widetilde{z}} + \boldsymbol{D} \frac{\partial c_{\text{gas}}}{\partial \widetilde{z}} \right) c_{\text{p},i} \frac{\partial T_{\text{gas}}}{\partial \widetilde{z}} \tag{17}
$$

The temperatures are a function of the position, $\widetilde{z}$, and time t. If isothermal conditions are assumed (e.g. temperature-controlled laboratory reactor or a very high dilution in an inert gas), which is done in the present work in order to keep consistency, and if the special geometric structure of the pellet is employed, one finds the dimensionless system

$$
\frac{\partial(\psi \boldsymbol{x})}{\partial \theta} = \frac{\partial}{\partial z} \left[\left(\beta^0 \frac{1}{\tau} (\psi \boldsymbol{x}) \boldsymbol{e}^T + \delta \frac{1}{\tau} \right) \frac{\partial(\psi \boldsymbol{x})}{\partial z} \right] + \frac{1}{\varepsilon} \sum_j^{n_R} \nu_j \omega_j \tag{18}
$$

in the gas phase and

$$
\frac{\partial(\psi \boldsymbol{x})}{\partial \theta} = \frac{\partial}{\partial z} \left(\delta \boldsymbol{S} \frac{1}{\tau} \right) \frac{\partial(\psi \boldsymbol{x})}{\partial z} + \frac{1}{1-\varepsilon} \sum_j^{n_R} \boldsymbol{\nu}_j \omega_j \tag{19}
$$

in the solid phase. The dimensionless quantities are defined as

$$
z = \frac{\widetilde{z}}{L} \tag{20}
$$

$$
\theta = \frac{t\Delta}{L^2} \tag{21}
$$

$$
\psi = \frac{p}{p|_{z=0.5}} \tag{22}
$$

$$
\omega = \frac{\widetilde{r} L^2 RT}{\Delta p|_{z=0.5}} \tag{23}
$$

$$
\beta^0 = \frac{r_P^2 p|_{z=0.5}}{8\eta\Delta} \tag{24}
$$

$$
\boldsymbol{\delta}^S = \begin{cases} \dfrac{D^S}{\Delta} & |i = j \\[2mm] 0 & |i \neq j \end{cases} \tag{25}
$$

$$
-\boldsymbol{\delta}^{-1} = \begin{cases} \dfrac{x_i \Delta}{D_{ij}} + \sum\limits_{\substack{l=1 \\ l \neq 1}}^{N} \dfrac{x_l \Delta}{D_{il}} + \dfrac{\Delta}{D_i^K} & |i \neq j \\[4mm] 0 & |i = j \end{cases} \times i \tag{26}
$$

The reaction rates $\widetilde{r}$ are not equal to the reaction rates r_R in Eqs. (11) and (12), since they are related to different control volumes. The term Δ denotes a specific diffusivity and $z = 0.5$ refers to the half diameter (outer radius).

The outer gas phase is described by a set of ODEs, if a cell model is employed one obtains for the bulk gas phase.

$$
\frac{d\boldsymbol{n}_R}{dt} = (\boldsymbol{x}_{\text{in}} - \boldsymbol{x}_R) \dot{n}_{\text{total,in}} - k \frac{p|_{z=0.5}}{RT} b
$$
$$
\times \left[(\boldsymbol{x}_R - \boldsymbol{x}|_{z=0.5}) - \boldsymbol{x}_R \sum_i^{n_c} (x_{R,i} - x_i|_{z=0.5}) \right] \tag{27}
$$

where the term x_R refers to the mole fraction in the reactor bulk gas phase.

This may be transformed into the dimensionless form

$$\frac{d\boldsymbol{x}_R}{d\theta} = \frac{1}{\theta_R}(\boldsymbol{x}_{in} - \boldsymbol{x}) - Bi\kappa$$
$$\times \left[(\boldsymbol{x}_R - \boldsymbol{x}|_{z=0.5}) - \boldsymbol{x}_R \sum_i^{n_c}(x_{R,i} - x_i|_{z=0.5}) \right] \quad (28)$$

with the Biot mass number

$$Bi = \frac{kL}{\Delta} \quad (29)$$

If the outer diffusion resistance is neglected the expression

$$\frac{dx_R}{d\theta} = \frac{1}{\theta_R}(x_{in} - x) - \kappa\varepsilon(1 - x_R\boldsymbol{e}^T)$$
$$\times \left(\beta\frac{1}{\tau}x\bigg|_{\widetilde{z}=L/2} \boldsymbol{e}^T + \frac{1}{\tau}\delta \right)\frac{\partial x}{\partial z}\bigg|_{\widetilde{z}=L/2} \quad (30)$$

will result.

In more complicated models for the reactor like dispersion models, the concentration profiles are given by a system of PDE. The system of equations describing the inside of the pellets (Eqs. (18) and (19)) is simply added as an additional dimension. This would increase the computational demand noticeably, because the time scales of the transport in the reactor and in the pellets are different.

The initial concentration profiles may be set arbitrarily. Often, an empty reactor is a useful approximation. The inert substances are present.

$$x_{gas}(t = 0) = x_{gas,0}, \qquad x_R(t = 0) = x_{R,0}, \qquad x_{solid} = 0 \quad (31)$$

The reactor and pellet gas phases are coupled by the mass transfer equations

$$Bi(x_R - x) = \frac{1}{\tau}(x\boldsymbol{e}^T + \delta)\frac{\partial x}{\partial z}\bigg|_{z=0.5} \quad (32)$$

if the film mass transfer resistance is taken into account, or

$$x\left(\widetilde{z} = \frac{L}{2}\right) = x_R \quad (33)$$

if it is neglected.

Similar equations can be found for the solid phase. If the surface diffusion is neglected ($\delta^S = 0$), Eq. (19) will become ODEs at the discretization points. So

$$\frac{\partial(\psi x)}{\partial\theta} = \frac{1}{1 - \varepsilon}\sum_j^{n_R}\nu_j\omega_j \quad (34)$$

is used at the boundary.

If a one-dimensional cell model is used, the input concentration may be equal to the outlet of the preceding cell.

$$x_{in,0} = x_{in,reactor}, \qquad x_{in,i} = x_{i-1} \quad (35)$$

Care must be taken of the reactor residence time, θ_R. The residence time is the first moment of the residence time distribution. The integral may not exist (e.g. in the case of irreversible adsorption). Therefore, a characteristic hydrodynamic residence time

$$t_r = \frac{n(t)}{\dot{n}_{in,0}} \quad (36)$$

is employed. The real hydrodynamic residence time of cell i is given by the correction

$$\theta_{R,i} = \theta_{R,i,0}\prod_{l=1}^{i-1}\left(1 + \sum_{j=1}^{n_R}\sum_{k=1}^{n_c}\nu_{jk}\omega_j\theta_{R,l}\right) \quad (37)$$

This is required, since the total residence time $\sum_i^{n_R}\theta_{R,i,0}$ should be independent of the number of cells. Otherwise, a different total residence time would be required if the number of cells is changed. Section 5 will show an application of the new technique.

5. Methane combustion

The total oxidation of methane on a commercial catalyst was investigated by the FR technique.

$$CH_4 + 2O_2 \rightarrow 2H_2O, \qquad \Delta H^{573} = -803 \text{ (kJ/mol)}$$

A commercially available catalyst, Envi Cat SC1219 (Solvay, Hannover), was used for the experiments. The particle size was 1–2 mm. The catalyst consists of 0.84 wt.% palladium on a γ-Al$_2$O$_3$ support. The palladium dispersion was 33.6% (measured by CO-Chemisorption) according to the manufacturer. The porosity of the support was measured to be 67% (from the density). The specific surface area is 217 m^2/g, measured by the BET-nitrogen isotherm method.

The exact preparation of the catalyst was unknown to the authors, but the palladium is oxidized to all appearances. After some experiments of the experiments the catalyst seems to be reduced. Before every experiment, the catalyst was used in the operating regime for several hours to minimize initial effects during the measurements.

The combustion of methanol and natural gas on palladium and palladium oxide has been investigated many times. The catalytic activity depends on the oxidation state. This was not always taken into account, so the mechanisms that were found are somewhat contradictory. A review is given by Golodets [51]. Generally, it is found that palladium, apart from platinum, is especially suitable for catalyzing the CH$_4$ combustion reaction. Rhodium, iridium, and ruthenium have a similar high activity. Gold, silver, copper, and nickel alloys are catalytically active, but their activity is lower, as it is known from early studies [52]. The experimental accuracy of the old measurements was relatively low.

Anderson et al. [53] have found by a pulse microcatalytic technique that supported catalysts of palladium and platinum on alumina are more active than metal oxide catalysts.
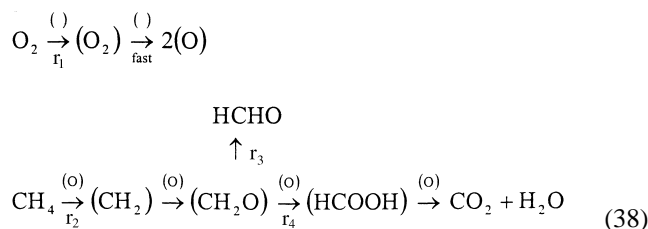
They found an activation energy of 92 kJ/mol and a reaction order of unity for methane. On the opposite, Kainz and Horwatitsch found that metal oxide catalysts may be as active as the noble metal catalysts [54]. Both groups did not determine the active surface areas at the catalysts. More precise measurements were done by Firth and Holland [55,56]. They employed a micro-calorimetric method and found a change of the activation energy from 138 to 50 kJ/mol at 563 K. The reaction order of methane is unity, the one of oxygen is zero (at 673 K).

The same reaction orders were found by Kambell for palladium–gold alloys [57]. These reaction orders my be explained, if the reaction of methane and chemisorbed oxygen is the rate-limiting step [58]. One should keep in mind that this is only one possible explanation. It is always dangerous to conclude the underlying mechanism from kinetic information.

Ahuja and Mathur [59] postulate a mechanism with non-dissociative adsorption of oxygen, methane, carbon dioxide, and water are also adsorbed. The surface reaction is the rate determining step.

Palladium(II)-oxide is also catalytically active. Elementary palladium is rapidly oxidized in an oxygen rich environment. Bulk palladium(II)-oxide is thermodynamically stable in the range of 523–1173 K [60]. Palladium oxide is, apart from trichrometetraoxide, especially active.

Cullis et al. [61] have investigated the methane combustion on a palladium alumina support catalyst that was oxidized during the reaction by a pulse method. They found formaldehyde as a by-product, but the catalyst had a high selectivity towards total oxidation. From measurements with different reactants they postulated a parallel-consecutive mechanism.

$$O_2 \xrightarrow[r_1]{(\ )} (O_2) \xrightarrow[fast]{(\ )} 2(O)$$

$$
\begin{array}{c}
HCHO \\
\uparrow r_3 \\
CH_4 \xrightarrow[r_2]{(O)} (CH_2) \xrightarrow[]{(O)} (CH_2O) \xrightarrow[r_4]{(O)} (HCOOH) \xrightarrow[]{(O)} CO_2 + H_2O
\end{array}
\tag{38}
$$

The following Eley–Rideal type kinetic expression may be derived from this reaction scheme.

$$r = k_2 p_{CH_4} \theta_o = \frac{k_1 k_2 p_{O_2} p_{CH_4}}{k_1 p_{O_2} + \nu k_2 p_{CH_4}},$$

$$\theta_o = \frac{(k_1/k_2)(p_{O_2}/p_{CH_4})}{\nu + ((k_1/k_2)(p_{O_2}/p_{CH_4}))},$$

$$r_{HCHO} = \frac{k_3/k_4}{(k_3/k_4) + \theta_o} r, \qquad r_{CO_2} = \frac{\theta_o}{(k_3/k_4) + \theta_o} r \tag{39}$$

The investigation of the mechanism may be supported by data from the oxidation of methane and other reactants on similar catalysts. These data may, for example, be found in the book of Golodets [51]. Since the present paper is on the FR technique, such examples are not listed here.

Cullis and Willat [62] have further investigated the methane oxidation on supported catalysts. They also found that the activation energy is halved at high temperatures. An important result is that the alumina support enhances the oxygen uptake, although the bare support adsorbs oxygen only after a careful desorption procedure. Another result is that the activation energy of different supported catalysts is the higher the more active components are impregnated.

Baldwin and Burch [63] have investigated the activity of different fresh catalysts in an oxygen-rich atmosphere. For the palladium–alumina support catalyst they found an increase of activity at the beginning of the reaction.

Foka et al. [64] give the following rate equation for an oxidized 0.2 wt.% PdAl$_2$O$_3$-catalyst.

$$r_{CH_4} = k_o \exp\left(\frac{-E_o}{T}\right) c_{CH_4}$$

$$k_o = (2 \pm 1.6 \times 10^{-5})10^8 \, (1/s),$$

$$E_o = (11.1 \pm 5 \times 10^{-3})kK$$

The influence of the products was investigated by Burch et al. [65]. They found that carbon dioxide as well as water inhibits the reaction. Water offsets the inhibition from carbon dioxide by the formation of stable hydroxyl groups on the surface. Above 723 K the influence of the products is negligible.

6. Experimental set-up

The schematic diagram of the laboratory set-up is shown in Fig. 1. It consists of a blending part for the reactants, a differential fixed-bed reactor with an external recycle, and an analysis part at the outlet. As feed gases methane 3.8, nitrogen 5.0 (Linde, Höllriegelskreuth), and synthetic air (20.5% oxygen, 79.5% nitrogen, manufacturer Messer Griesheim, Frankfurt a.M.) are used. The pressure is reduced to 5 bar by common reducing valves. In the blending unit, the gases are fed into the reactor by a combination of thermal mass flow controllers (types and manufacturers: for methane 1259C-00260 SV by MKS Instruments, Munich, for nitrogen, F-231C-FA-33-V by Bronkhorst High-Tech, Ruurlo, for synthetic air WFCO22 by Manger + Wittmann, Garching) and three-way solenoid valves (Bürkert, Ingelfingen). The latter ones are used for generating step signals in order to compensate for the transient behavior of the flow controller. For safety reasons, additional cut off solenoid valves are included in every channel (also by Bürkert, Ingelfingen), and the synthetic air is fed into the reactor independent from the mixture of methane and nitrogen. With this combination of mass flow controllers and valves, any continuous variation of the input flows and composition can be generated. Additionally, pulses and step signals can be created. The mass flow controllers and valves are connected to a personal computer which can generate the desired input signals. In the
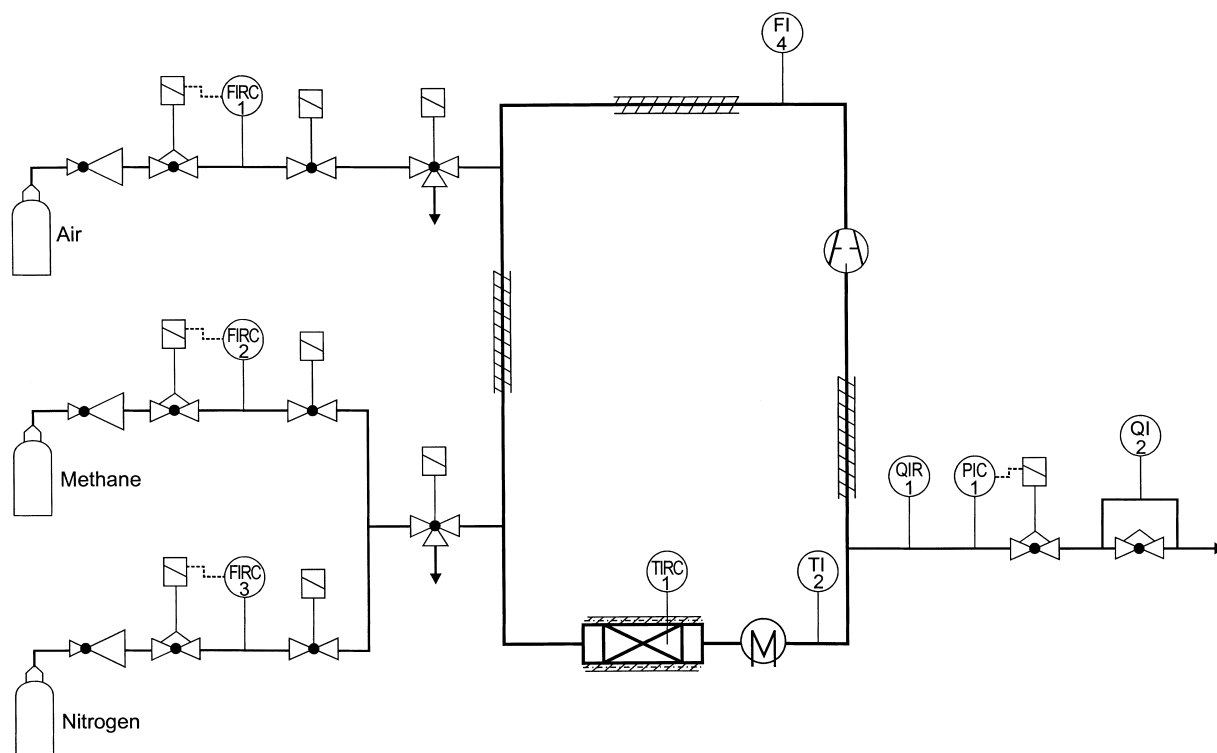
Fig. 1. Flow sheet of the experimental set-up, details on the equipment are given in the text.

present experiments one reactant (oxygen, air) flows at a constant rate into the differential reactor while the flow rate of methane and nitrogen are sinusoidally varied such that the total gas flow rate is constant, that means an increase in the methane flow rate is accompanied by a decrease of the nitrogen flow rate.

The recycle reactor consists of a tube reactor ($\varnothing$ 14 mm, length 10 cm) filled with the catalyst, a vane compressor (GK07M, ASF Thomas, Memmingen) with outlet filter (Nupro, Solon, OH) and a thermal mass flow meter (F-112AC-HA-33-V, Bronkhorst High-Tech, Ruurlo). The reactor is placed in a metal heat bath (MV85/ER, Gestigkeit, Düsseldorf) filled with 6000 nuts M5, DIN935, brass) to keep the desired temperature. The reaction mixture is cooled down in a double-pipe heat exchanger after having left the fixed bed, because the operating temperature of the pump is restricted to 80°C or less. A 1:1 water–ethylene glycol mixture is used as coolant, which is kept at a fixed temperature by a combination of a once-through cooler and a temperature controller (DLK15 and K6, both Dr. R. Wobser, Lauda–Königshofen). The cooling temperature can be set between −15 and 80°C. In front of the reaction tube, the mixture is heated by a heating band (Horst, Lorsch).

Type K thermocouples (Thermo-Electric, Colonia) are built in at two positions, at the end of the fixed bed and after the cooler. The pressure in the reactor is regulated by an electronic pressure controller (P-702-FA-33-V, Bronkhorst High-Tech, Ruurlo). The outlet gas is on-line analyzed by a mass spectrometer (type MSD-5972a connected to a

6890GC, both Hewlett Packard, Waldbronn). An additional gas chromatograph (GC8A, Shimadzu, Duisburg) is available for substance identification and as a quantitative reference. For the present measurements the gas chromatograph is used only for the calibration of the mass spectrometer. All electronic input signals are recorded by a PC (instrumentation hardware and software by Strawberry Tree, Sunnyvale), which also generates the control signals. The typical operating conditions are in the temperature range from 260 to 920 K and in the pressure range of 0–10 bar. All parts are made of stainless steel. For the connections, tube fittings (Swagelok, Solon) are used.

A reactor with an internal recycle (Berty type) turned out to be inappropriate, since the mixing was not efficient at the low pressure (1130 mbar). At higher pressures the use of a reactor with an internal recycle may be more advantageous due to the lower dead volume. The present set-up has a total volume of 1.1 l with a fixed-bed volume of 12.5 ml.

6.1. Steady state reaction rate

At first, the steady state reaction rate equation was determined. The reactor pressure was set to 1130 mbar, 9.9675 g of catalyst were employed. A number of 110 valid data points were measured for the kinetic expressions. At every point the outlet composition was monitored until the steady state was obtained. The temperature range covered 530–690 K. The volume fraction of methane in the feed varied between 2 and 14%, the oxygen fraction between 4 and

20%. The resulting volume fractions measured in the reactor were 0–17% O_2, 0–15% CH_4, 0.5–9.6 and 0.2–4% H_2O. The measurement of water volume fractions was subject to severe errors, so the reaction rates were corrected to the dry mixture and the water fraction was calculated from the stoichiometry of the reactions for the fitting procedure.

A fitting procedure was afterwards used for determining the parameter sets for various kinetic expressions. The best fit could be obtained for a Langmuir–Hinshelwoord type equation.

$$r = \frac{A_0 \exp(-E_0/RT) K_{O_2} K_{CH_4} P_{O_2} P_{CH_4}}{(1 + K_{O_2} P_{O_2} K_{CH_4} P_{CH_4} + K_{CO_2} P_{CO_2})^2} \tag{40}$$

with the parameters

$A_0 = 4040\,(\text{mmol/min}\,g_{cat})$, $\qquad K_{O_2} = 65\,400\,(1/\text{Pa})$,

$K_{CH_4} = 132\,000\,(1/\text{Pa})$, $\qquad E_0 = 52.700\,(\text{kJ/mol})$,

$K_{CO_2} = 9020\,(1/\text{Pa})$

The variables A_0, E_0, and the adsorption constants, K_i, were fitted according to a least-squares fit over the entire temperature and partial pressure range. The activation energy describes the temperature dependence of all parameters within the experimental range. The same holds for the Eley–Rideal mechanism. Assuming an Eley–Rideal type mechanism with adsorbed oxygen leads to the kinetic expression

$$r = \frac{A_0 \exp(-E_0/RT) K_{O_2} P_{O_2} P_{CH_4}}{1 + K_{O_2} P_{O_2} + K_{H_2O} P_{H_2O} + K_{CO_2} P_{CO_2}} \tag{41}$$

with

$A_0 = 2.3 \times 10^6\,(\text{mol/min}\,g)$, $\qquad E_0 = 159\,(\text{kJ/mol})$,

$K_{O_2} = 6 \times 10^4\,(1/\text{Pa})$, $\qquad K_{H_2O} = 1.7 \times 10^6\,(1/\text{Pa})$,

$K_{CO_2} = 1.7 \times 10^6\,(1/\text{Pa})$

This equation gave a considerably higher residual in the parameter search (0.0298 compared to the Langmuir–Hinshelwood type (0.0192)). Especially doubtful is the high activation energy, a fit of selected reaction rates to a potential expression gave an activation energy of 58 kJ/mol.

6.2. Adsorption constants

For a more precise investigation of the elementary steps, the linear adsorption constant of methane and oxygen were determined by the chromatographic method proposed by Schneider and Smith [66]. The adsorption constants measured by this method are only used for a better understanding of the adsorption properties of the components. The values are not used in the final microkinetic expression. The experiments were executed by means of a gas chromatograph. The following assumptions were made:

- the gas and the adsorbed phase are in equilibrium;
- the coverages are small, the adsorption isotherm is linear;
- the bed is isothermal, the pressure is constant in the entire column;
- the pellets are spherical.

This method relates the moment of the output signal of a pulse input to a chromatographic column filled with the catalyst to the linear adsorption constant.

$$\mu_1' = \frac{2}{v}\left(1 + \delta_0 + \frac{t_{0,A}}{2}\right) \tag{42}$$

$$\delta_0 = \frac{1 - \varepsilon_p}{\varepsilon_p}\varepsilon_b\left(1 + \frac{\rho_p}{\varepsilon_b}\right)K_A \tag{43}$$

where z is the length of the column, v the gas velocity, $t_{0,A}$ the injection time, ε_p and ε_b the pellet and bed porosities, and K_A the desired adsorption constant. Since the employed gas chromatograph does not directly give the feed onto the column, a dead moment $\tilde{\mu}_1$ was determined first. For the procedure, used catalyst was ground and a fraction of 200–500 µm was fed into a column of 1.95 m length. A HP6890 chromatograph was used for the measurements. The moments for methane were determined at different temperatures, and the resulting adsorption constants were calculated. The results are given in Table 1.

The method could not be applied to the oxygen adsorption on the reduced catalyst, because oxygen did not desorb but formed palladium oxide. Thus the catalyst was oxidized by subsequent pulses of oxygen, until the size and shape of the oxygen peaks at the outlet remained constant. The linear adsorption constant was then determined for the oxidized catalyst. It is noteworthy, that we could not determine the methane adsorption constants for the oxidized catalyst, because methane would react with the bulk oxygen. The results are presented in Fig. 2.

Oxygen adsorbs in two forms: in a surface form as well as in a bulk form. So the determination of a linear adsorption constant is very erroneous. The values given here may be considered as a limiting case for infinite dilution and very

Table 1
Adsorption constants of methane on palladium and oxygen on palladium oxide

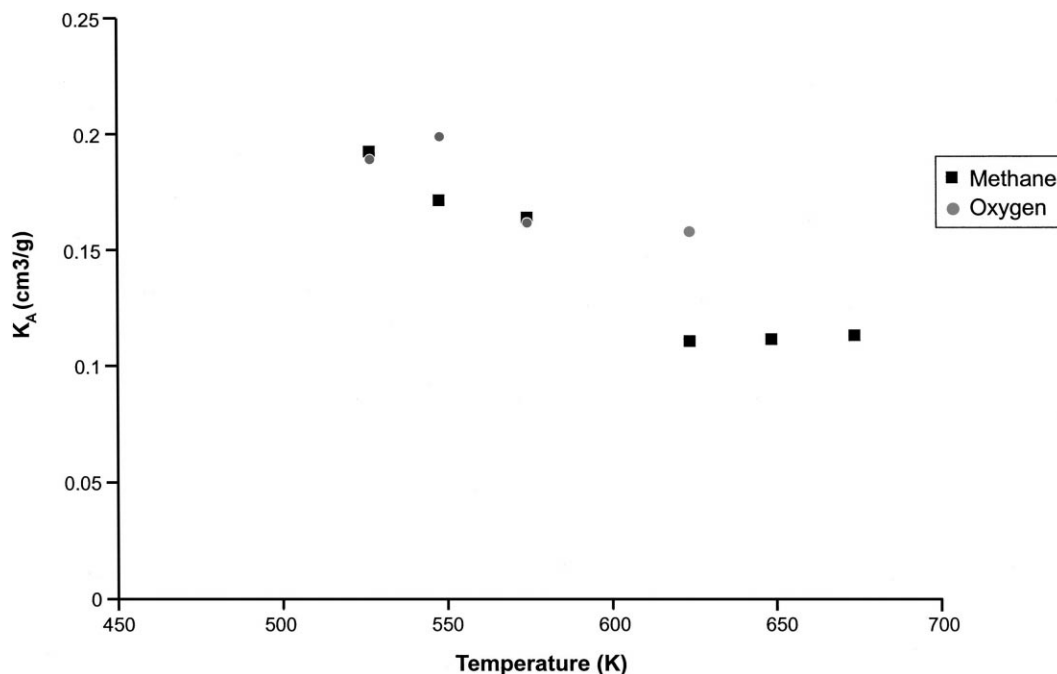| T (°C)	K_A (cm^3/g)
Methane	
250	0.192
275	0.174
300	0.164
325	0.078
350	0.111
375	0.111
400	0.112
$\Delta H_{ads} = -12\,147$ J/kg	
Oxygen	
250	0.18946
250	0.19808
300	0.16228
350	0.15801
$\Delta H_{ads} = -5924$ J/kg	

Fig. 2. Adsorption constants of methane on the reduced catalyst (squares) and oxygen on the oxidized catalyst.

short time. So they are valid for most surface oxygen. The heats of adsorption, which we determined in this work, again indicate that the methane adsorption is much stronger than the adsorption of surface oxygen. The ratio of the adsorption strengths is considerably shifted to methane at elevated temperatures.

6.3. Determination of the frequency response

The FRs of the system were measured for different temperatures and feed compositions in single frequency experiments. Before the measurements, the catalyst was used for several days at different operating conditions to minimize

initial effects. The method was used in a range that covers the reduced as well as the oxidized state of the catalyst, both states are employed during the pretreatment. Several reduction and oxidation processes took place before the catalyst was used for the experiments.

At the beginning of each measurement, the operating temperature, recycle flow, residence time, and mean feed composition were set. As soon as the steady state was obtained, the feed is switched to a sinusoidally oscillating methane composition. Before every single frequency a periodical operation is hold for at least 10 min. The output signal is then measured for 12 periods, at least for 10 min. Operating parameters are given in Table 2. The frequency range of the

Table 2
Operating parameters of the FR measurements

Measurement	t_r (s)	$T_{reactor}$ (°C)	$\dot{V}_{methane}$ (ml_n/min)	$A_{methane}$ (ml_n/min)	$\dot{V}_{air}$ (ml_n/min)
A	9.70	356.0	49.8	33.8	151.1
B	3.50	354.1	49.9	33.8	151.2
C	3.70	280.8	50.0	33.7	151.2
D	5.45	281.8	49.8	33.9	150.9
E	7.00	283.2	49.7	33.8	151.0
F	4.06	215.1	49.8	33.8	151.1
G	4.07	211.3	49.9	16.8	150.9
H	4.00	218.2	66.3	68.0	151.2
J	4.00	206.0	49.8	16.9	151.1
K	5.49	266.3	32.7	17.0	308.6
L	9.71	267.7	32.9	16.8	308.5
M	3.87	261.2	32.7	17.1	308.7
N	5.46	272.3	15.9	8.8	308.8
O	9.59	269.0	15.9	8.8	308.8
P	5.50	272.8	49.8	17.0	308.8
Q	9.72	279.0	49.9	16.8	308.5

system was chosen from the experimental relative output/input amplitude. At a period time of 5 min or longer, all processes are quasi steady-state, i.e. a steady-state kinetic expression is suitable for the description. The shortest period time employed is 10 s. The relative amplitude is very low then, i.e. the oscillations are damped due to the backmixing in the reactor. If even faster processes are to be investigated, a lower reactor volume is required.

For the evaluation, the composition of the reaction mixture is measured. The composition of the feed is calculated from the output signal of the mass flow controllers.

6.4. Evaluation of data

The amplitude response can be determined from the ratio of the first Fourier coefficients of the reactor and input signals.

$$A(\omega) = \frac{a_{1,R}}{a_{1,in}} \tag{44}$$

where the indices R refers to the reactor outlet.

From the amplitude response, the parameters of Eq. (7) are determined by a least-squares-fit. From these, the parameters κ_R and τ_a (see Eqs. (4)–(10)), that are describing the reaction behavior, can be calculated. Some results are shown in Table 3.

After the results from the linear model (Eqs. (7) and (8)), the parameters for a non-linear model (Eqs. (11) and (12)) were determined. A Langmuir–Hinshelwood mechanism was proposed

$$CH_4 + ()\underset{r_{-1}}{\overset{r_1}{\rightleftarrows}}(CH_4), \qquad O_2 + ()\underset{r_{-2}}{\overset{r_2}{\rightleftarrows}}(O_2),$$

$$(CH_4) + 2(O_2)\overset{r_3}{\rightarrow}CO_2 + 2H_2O \tag{45}$$
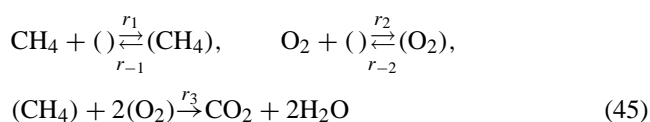
with the rate equations.

Table 3
Kinetic constants for the linearized model

Measurement	K	T_E (s)	τ_a (s)	κ_R (1/s)
A	0.98588	125.34	20.23	0.00071
B	0.83641	66.27	12.61	0.01551
C	0.92821	72.33	12.40	0.00624
D	0.96070	90.23	14.95	0.00274
F	0.97471	76.27	12.45	0.00208
G	0.97229	76.95	12.60	0.00226
M	0.85819	73.52	13.63	0.01212
N	0.59821	36.39	9.68	0.06938
Q	0.98479	124.45	20.11	0.00077

$$r_1 = k_1 C_{CH_4}C_{()}, \qquad r_2 = k_2 C_{O_2} C_{()},$$
$$r_3 = k_3 C_{(CH_4)}C_{(O_2)}, \qquad r_{-1} = k_{-1}C_{(CH_r)},$$
$$r_{-2} = k_{-2}C_{CO_2} \tag{46}$$

The constants k_1–k_{-2} as well as c_0 and t_r were determined, whereby the error criterion was the least squares-error of the sum of the zeroth and first Fourier coefficients of methane and oxygen. The results are shown in Table 4. The data sets in Table 4 refer to the corresponding operation conditions in Table 2.

7. Discussion of the results

It can be taken as a fact that palladium is catalytically active in the reduced state as well as in the oxidized state [51]. An important result of these experiments is that these two different oxidation states may be described by a single kinetic model. A practical application for the reaction under varying conditions might be the treatment of exhaust gases with varying oxygen content.

The reduced catalyst takes up oxygen in two ways, as bulk oxygen in a chemisorbed form (by oxidation) and as a reversibly adsorbed molecular species.

Table 4
Kinetic constants for the Langmuir–Hinshelwood reaction scheme

Measurement	k_1 (10^5 m^3/(mol s))	k_2 (10^5 m^3/(mol s))	k_3 (10^{-5} m^3/(mol s))	k_{-1} (10^2 l/s)	k_{-2} (10^2 l/s)	c_{act} (10^2 mol/m^3)
A	9.40	8.92	3.13	4.99	1.18	7.13
B	11.4	12.0	3.18	5.61	1.57	7.22
C	11.3	10.7	11.2	5.92	2.60	2.06
D	11.6	13.2	5.34	5.13	1.61	3.05
E	9.23	7.18	4.71	4.83	1.60	4.08
F	6.07	12.3	20.4	3.40	8.78	1.61
G	3.45	2.85	12.4	2.69	0.701	1.80
H	91.2	274	242	9.12	68.4	12.4
J	9.37	8.87	3.02	4.75	1.12	11.9
K	9.17	8.81	16.9	4.73	9.08	2.14
L	8.16	8.01	14.4	4.26	8.37	2.30
M	8.42	7.44	13.4	4.20	7.43	2.38
N	9.02	7.40	19.3	4.18	6.87	2.12
O	9.12	11.0	27.5	4.79	11.6	1.66
P	9.43	9.43	7.73	4.72	5.72	3.46
Q	9.43	9.41	7.72	4.72	5.72	3.55

7.1. Adsorption measurements

One must keep in mind that the adsorption constants for methane and oxygen refer to different oxidation states. With the method employed, it is impossible to determine the constants for both oxidation states, because the catalyst will change its state during the measurements. In principle the surface diffusion coefficients can be calculated from the chromatographic measurements [67], but an evaluation only revealed that these are very small.

It is conspicuous that the adsorption constants of both reactants are comparable in magnitude for every temperature (see Table 1). The heats of adsorption are relatively small, so the adsorption seems to be weak. The heat of adsorption for oxygen refers to a state which is nearly saturated. So, one may conclude that it is very unlikely that oxygen will limit the catalytic reaction on the oxidized catalyst. Strongly and weakly bound oxygen can be converted into each other easily, so it is not important for a kinetic investigation, which of the two species participates in the surface reaction, because they can be taken as a supplier to each other. However, the adsorption kinetics for the physisorption may be the rate determining step. This cannot be found from the adsorption constants.

7.2. Steady state kinetic expression

The measured data may be described better by a Langmuir–Hinshelwood type than by an Eley–Rideal type rate equation. The activation energy of the Eley–Rideal type expression differs considerably from the data in the literature and the values in the Langmuir–Hinshelwood expression. So we believe that it has no physical basis. From an oral information of the manufacturer there is a danger of a sudden exothermic reaction, if the catalyst is loaded at ambient temperature and oxygen is fed continuously during the heating-up phase. This behavior cannot be explained easily by an Eley–Rideal mechanism, so we claim from this information that methane should be treated as an adsorbed species.

It is noteworthy that the adsorption constant of the rate equation is much higher for methane than for oxygen. This may not be due to a real physical difference in the adsorption behavior, but it may be due to the fact that the regardable influence of methane is higher in the experimental range.

Since the production of water and carbon dioxide are coupled in the experiment, their influence cannot be decoupled in the present rate equation. The Eq. (39) should not be employed without further investigations for the description of systems with a significantly different ratio of water and carbon dioxide than in a combustion reaction.

7.3. Linear model

Some results are noteworthy. No simple relation (e.g. an experimental function) between the rate constant, κ_R and the temperature can be found (Fig. 3). This also holds if only the reduced or the oxidized state is taken into account. The apparent residence time τ_a decreases with the hydrodynamical residence time, $t_r = n/\dot{n}$ as it is expected (Fig. 4). The apparent residence time τ_a is much larger, the ratio τ_a/t_r lies between 1.7 and 3.5 (Fig. 5). This is independent of the temperature and the oxidation state of the catalyst.

The experimental reproducibility for the composition measurement by mass spectrometry and thus the underlying data was determined to 5%. These results indicate that an important influence to the kinetic expression must have been omitted. With respect to the experimental conditions the most important variable is the oxygen content of the reaction mixture. The authors suspect that the oxygen partial
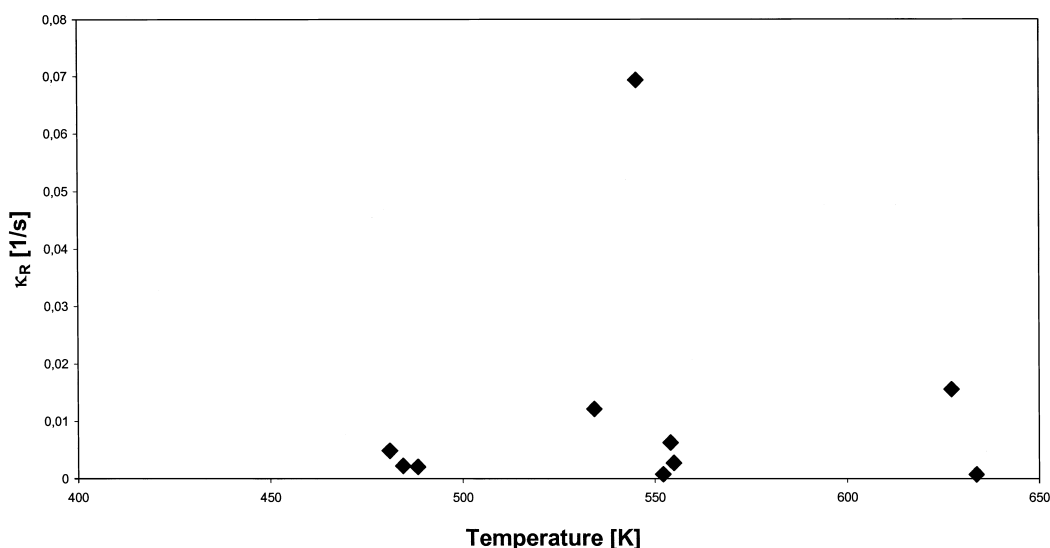

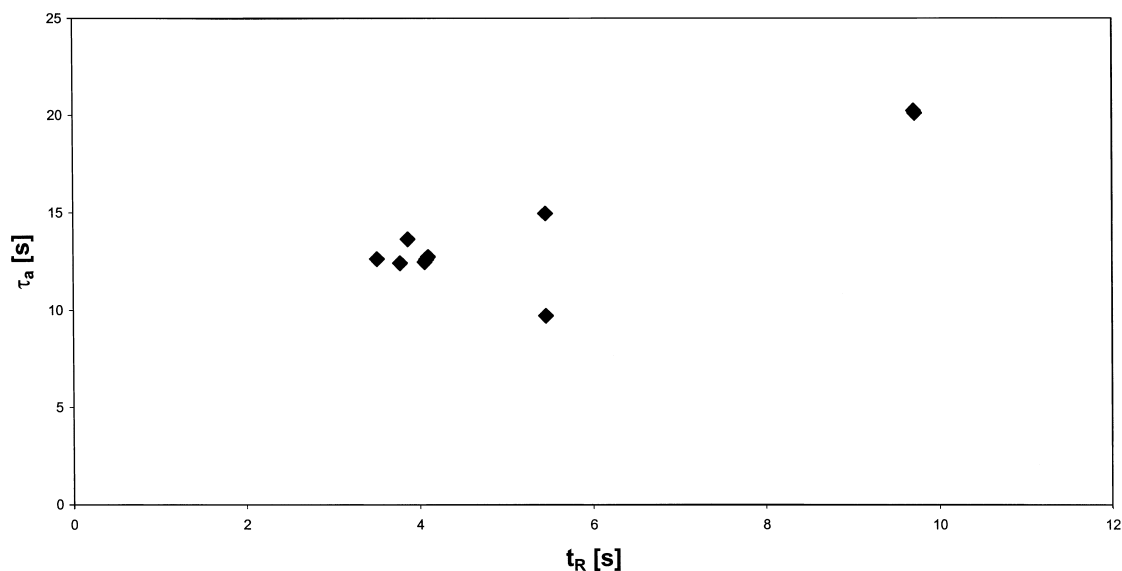Fig. 3. Reaction rate constants for the linear model.

Fig. 4. Comparison of the hydrodynamical and the apparent residence time in the linear model.

pressure is more important than in the steady state (other authors postulate a reaction order of zero). In the derivation a zeroth reaction order was assumed.

A source of error comes from the fact that, only the first Fourier coefficient was employed for the parameter fit while the zeroth coefficient, that includes much information about the conversion, was omitted. In linear models this is required in the evaluation, if the non-stationary behavior is to be included.

7.4. Microkinetics

The Langmuir–Hinshelwood reaction scheme (Eq. (45)) allows for the qualitative explanation of all experimen-

tal observations, which is not possible by an Eley–Rideal scheme. In order to verify the parameter sets, the optimization was repeated from different starting points. The results were reproduced several times. As the adsorption and desorption processes are relatively fast, it is not possible to verify the elementary sorption kinetic constants k_1, k_2, k_{-1}, k_{-2} by this method, rather the adsorption 'equilibrium' constants k_1/k_{-1}, respectively, k_2/k_{-2} are the critical values besides the surface reaction rate constant k_3.

The determining parameters for the reaction rate constants are the temperature and the oxidation state of the catalyst. The oxidation state is given by the ratio $\dot{n}_{methane,in}/\dot{n}_{oxygen,in}$ in the periodical case. The difference to the stoichiometric
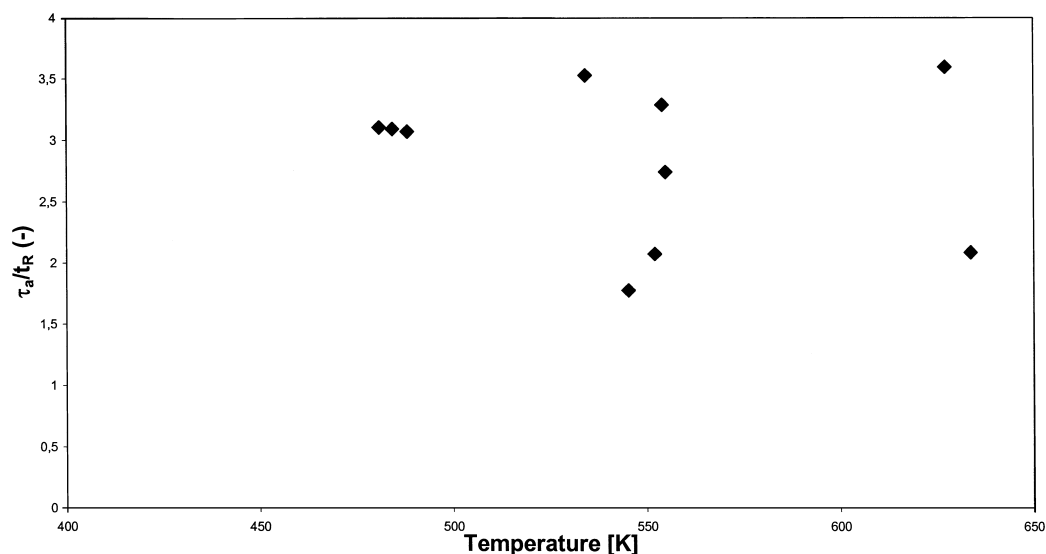

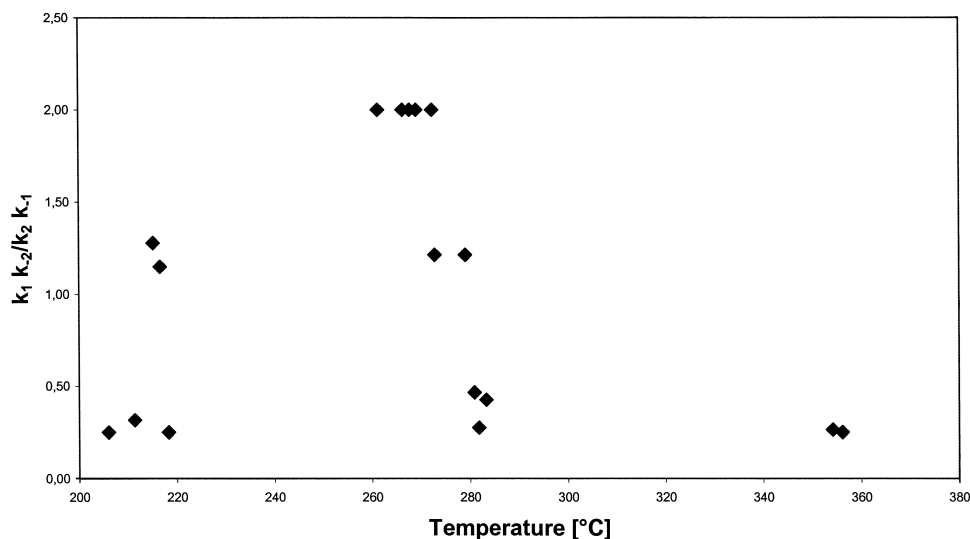Fig. 5. Temperature dependency of the adsorbed amount in the linear model.

Fig. 6. The ratio of the equilibrium adsorption constants as a function of temperature.

ratio $\dot{n}_{\text{methane,in}}/\dot{n}_{\text{oxygen,in}} = 2$ is an indicator to the oxidation state. This applies the mean value as well as phases within the period. If the ratio is higher than the stoichiometric ratio, the catalyst is totally reduced. The investigation shown here is on the oxidized catalyst, only one measurement (H, see Tables 2 and 4) was made in the range. During all other measurements methane was below the stoichiometric ratio averaged over time, although oxygen was below the stoichiometric ratio at a part of the period in some measurements. The catalyst is partially reduced during these experiments.

If the dependency of the kinetic constants on temperature and oxidation state is evaluated, the influence of the temperature is much smaller than the influence of the oxidation state. The ratio of the adsorption 'equilibrium'

constants

$$\frac{K_{\text{ads,CH}_4}}{K_{\text{ads,O}_2}} = \frac{k_1 k_{-2}}{k_2 k_{-1}}$$

is shown as a function of temperature in Fig. 6. There is no simple dependency. The same ratio as a function of the oxidation state (Fig. 7) shows that the adsorption 'equilibrium' is shifted to oxygen as the catalyst is reduced. The surface reaction rate constant k_3 also depends on the oxidation state (Fig. 8). It is noticeable that the reduced catalyst has an activity that is an order of magnitude higher compared to the oxidized catalyst (this was verified qualitatively by a step-response experiment). On the other hand, the activity of the oxidized catalyst decreases by partial reduction.
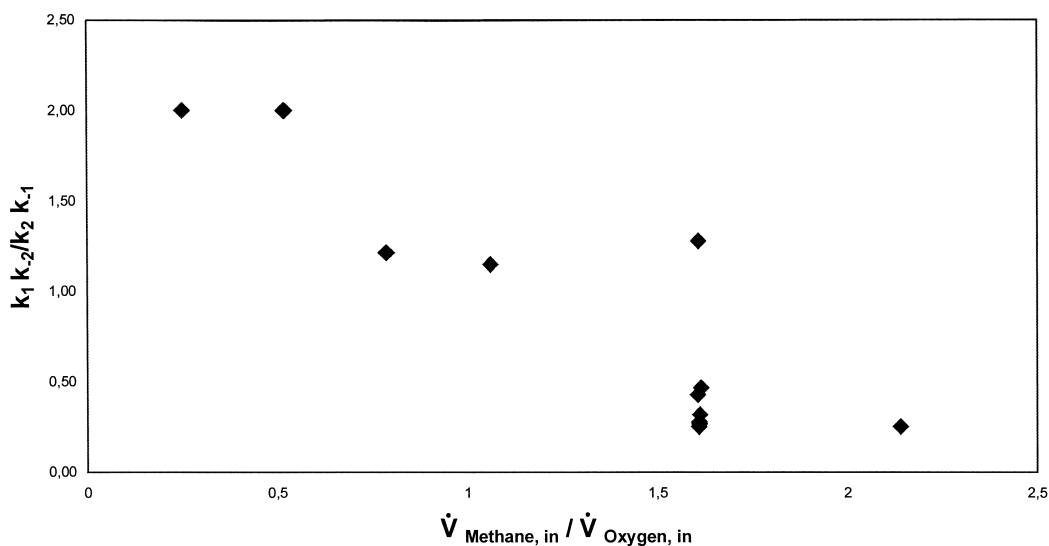

Fig. 7. The ratio of the equilibrium adsorption constants as a function of the oxygen state of the catalyst.
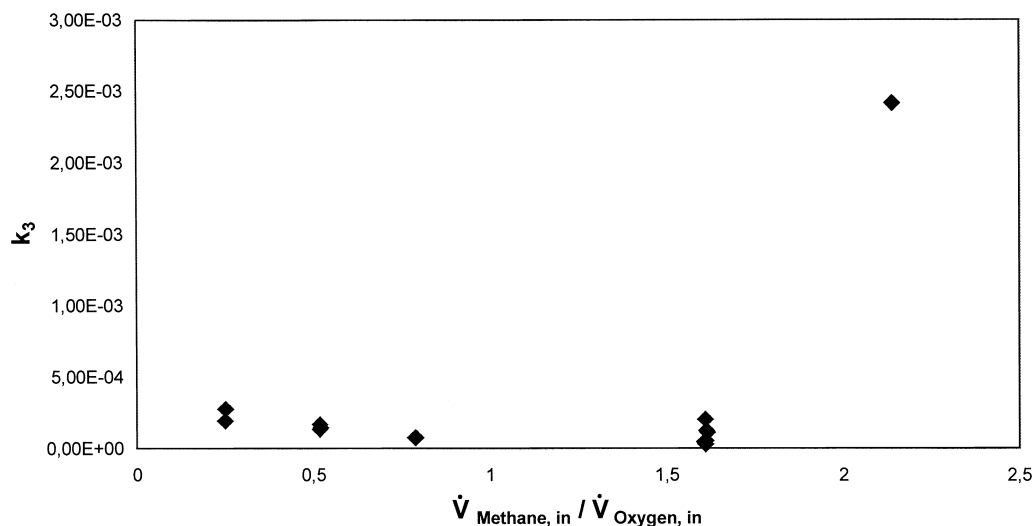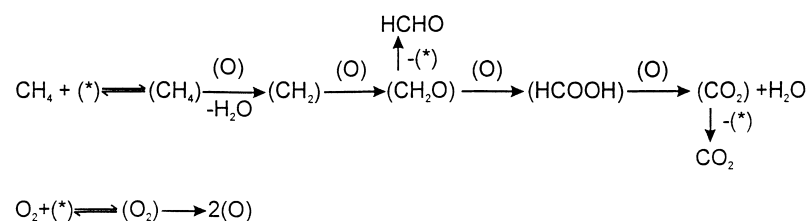
Fig. 8. The surface reaction constant as a function of oxygen state.

These parameter sets show the various problems that occur during the development of a kinetic scheme for the non-stationary operation. From the analysis of the present data it is straight-forward to fit the kinetic parameters as a function of two variables, temperature and oxidation state. But, if the resulting kinetic expressions is to be used for the description of non-stationary thermal effects, it is necessary, to employ a non-isothermal operation during the experiments for a reliable expression. One should keep in mind that the present experiments were done at various temperatures, but isothermally at each temperature level.

A mechanism may also postulated. In combination with the results of Ahuja and Mathur [59], the following scheme may explain all results.

Depending on the desired accuracy different models may be used. A linear model is useful for getting initial values for a more detailed model or for time-critical applications, e.g. an on-line optimization of a production plant. More complicated models may cover a wider range of applications and may be used for finding hints to the underlying mechanism. Two models are presented here, a homogeneous model, which may be employed for a parameter optimization and a more rigorous model that also includes non-homogeneous profiles within the catalyst pellets, which is used for the verification only, since the computational demand is very high. If sufficiently fast computers become available in the future, the rigorous model may also be used for a parameter optimization. This may be useful, if catalyst restructurations become important in the transient behavior.

$$CH_4 + (^*) \rightleftharpoons (CH_4) \xrightarrow[-H_2O]{(O)} (CH_2) \xrightarrow{(O)} (CH_2O) \xrightarrow{(O)} (HCOOH) \xrightarrow{(O)} (CO_2) + H_2O$$

with the $HCHO$ via $-(^*)$ above (CH_2O), and (CO_2) going down via $-(^*)$ to CO_2.

$$O_2 + (^*) \rightleftharpoons (O_2) \longrightarrow 2(O)$$

Oxygen is activated in a two step mechanism, with the physisorption as the rate determining step. The methane oxidation is via several intermediates. The physisorption of both reactants is concurring. The experiments clearly support the Langmuir–Hinshelwood mechanism.

8. Conclusions

The frequency-response method offers a technique for the determination not only of the steady-state kinetics but also of characteristic time constants.

The new technique has been employed for the investigation of the catalytic combustion of methane on a palladium support catalyst. A Langmuir–Hinshelwood mechanism was found. The microkinetic rate constants were determined. This depends mainly on the oxidation state of the active component. The reduced catalyst is more active. Furthermore, this unique method offers the possibility to determine the capacity of catalytically active sites as well as the adsorption constants for highly reactive intermediate states. For the further development of the new method, a non-isothermal operation in the experiments is in preparation.

References

[1] K. Muralidhar, D. Mishra, Determination of dispersion coefficients in a porous medium using the frequency response method, Exp. Heat Trans. 10 (1997) 109–118.

[2] R.M. Asadullin, Number of solutions in the inverse problem of nonstationary chemical kinetics, Theor. Foundam. Chem. Eng. 32 (1998) 136–141.

[3] G.A. Somorjai, Introduction to Surface Chemistry and Catalysis, Wiley, New York, 1994.

[4] M. Boudart, Kinetics on ideal and real surfaces, AIChE J. 2 (1956) 62–64.

[5] S. Kiperman, K.E. Kumbilieva, L.A. Petrov, Classical catalytic kinetics — what is the point of the matter? Ind. Eng. Chem. Res. 28 (1989) 376–379.

[6] H.M. Hulburt, Y.G. Kim, Reaction mechanisms for engineering design, Ind. Eng. Chem. 58 (1966) 20–31.

[7] K. Tamaru, Dynamic Heterogeneous Catalysis, Academic Press, New York, 1978.

[8] H. Kobayashi, M. Kobayashi, Transient response method in heterogeneous catalysis, Catal. Rev.-Sci. Eng. 10 (1974) 139–176.

[9] C.O. Bennett, The transient method and elementary steps in heterogeneous catalysis, Catal. Rev.-Sci. Eng. 13 (1976) 121–148.

[10] P. Biloen, Transient kinetic methods, J. Mol. Cat. 21 (1983) 17–24.

[11] T. Furusawa, M. Suzuki, J.M. Smith, Rate parameters in heterogeneous catalysis by pulse techniques, Catal. Rev.-Sci. Eng. 13 (1976) 43–76.

[12] A. Renken, Instationary reactor operation for the modeling of heterogeneous catalytic reactions, Chem.-Ing.-Tech. 62 (1990) 724–733 (in German).

[13] A. Renken, R. Doepper, M. Schmid, Application of non-stationary and periodic processes in the study of heterogeneous catalytic kinetics, in: G. Sandstede, G. Kreysa (Eds.), Instationary Processes and Dynamic Experimental Methods in Catalysis, Electrochemistry and Corrosion, Vol. 120, Dechema-Monographie, VCH, Weinheim, 1989, pp. 273–290.

[14] R. Doepper, A. Renken, Dynamic experimental methods using in situ measurements of the surface intermediates applied to the fine chemistry, Chimia 50 (3) (1996) 61–64.

[15] H. Hofmann Dynamic experiments for the analysis of complex heterogeneous catalytic reaction Chem.-Ing.-Tech. 62 (1990) 31–46 (in German).

[16] K. Tamaru, Dynamic relaxation methods in heterogeneous catalysis, in: J.R. Anderson, M. Boudart (Eds.), Catalysis — Science and Technology, Vol. 9, Springer, New York, 1991, pp. 87–129.

[17] P.L. Mills, J.J. Lerou, Transient response methods for assisted design of gas phase heterogeneous catalysts: experimental techniques and mathematical modeling, Rev. Chem. Eng. 9 (1993) 1–96.

[18] V.N. Pisarenko, Analysis and modeling of catalytic processes, Theor. Foundam. Chem. Eng. 31 (1998) 398–414.

[19] S.W. Weller, Kinetics of heterogeneous catalytic reactions, Catal. Rev.-Sci. Eng. 34 (1992) 227–280.

[20] A. Garayhi, F.J. Keil, Measurement methods for the investigation of chemical kinetics under instationary conditions, Chem. Tech. (Leipzig) 52 (2000) 80–89 (in German).

[21] F.J. Keil, Development of microkinetic expressions by instationary methods, submitted for publication.

[22] J.T. Gleaves, J.R. Ebner, T.C. Kuechler, Temporal analysis of products (TAP) — a unique catalyst evaluation system with submillisecond time resolution, Catal. Rev.-Sci. Eng. 30 (1988) 49–116.

[23] S.L. Shannon, J.G. Goodwin Jr., Charakterisation of catalytic surfaces by isotopic transient kinetics during steady-state reaction, Chem. Rev. 95 (1995) 677–695.

[24] J. Dumesic, D.F. Rudd, L.M. Aparicio, J.E. Rekoske, A.A. Trevino, The Microkinetics of Heterogeneous Catalysis, ACS Professional Reference Book, ACS, Washington, 1993.

[25] K.C. Waugh, Prediction of global reaction kinetics by solution of the Arrhenius parameterized component elementary reactions: microkinetic analysis, Catal. Today 53 (1999) 161–176.

[26] P. Stoltze, Microkinetic simulation of catalytic reactions, Prog. Surf. Sci. 65 (2000) 65–150.

[27] F. Leder, J.B. Butt, The dynamic behavior of a fixed-bed catalytic reactor, AIChE J. 12 (1966) 1057–1063.

[28] Y.-E. Li, D. Willcot, R.D. Gonzalez, Determination of rate constants by the frequency response method: CO on Pt/SiO$_2$, AIChE J. 35 (1989) 423–428.

[29] D.T. Lynch, N.P. Walters, Frequency response characterization of reaction systems: external recycle reactor with a solid adsorbent, Chem. Eng. Sci. 45 (1990) 1089–1096.

[30] J.R. Schrieffer, J.H. Sinfelt, Frequency response analysis of surface reactions in flow systems, J. Phys. Chem. 94 (1990) 1047–1050.

[31] Y. Yasuda, Frequency response method for study of the kinetic behaviour of a gas-surface system: 1. Theoretical treatment, J. Phys. Chem. 80 (1976) 1867–1869.

[32] Y. Yasuda, Frequency response method for study of the kinetic behaviour of a gas-surface system: 2. An ethylene-on-zinc oxide system, J. Phys. Chem. 80 (1976) 1870–1875.

[33] Y. Yasuda, M. Saeki, Kinetic details of a gas-surface system by the frequency response method, J. Phys. Chem. 82 (1978) 74–80.

[34] Y. Yasuda, Frequency response method for the study of kinetics of a heterogeneous catalytic reaction of gases, J. Phys. Chem. 93 (1989) 7185–7190.

[35] Y. Yasuda, Frequency response method for study of kinetic details of a heterogeneous catalytic reaction of gases: 1. Theoretical treatment, J. Phys. Chem. 97 (1993) 3314–3318.

[36] Y. Yasuda, K. Nomura, Frequency response method for study of kinetic details of a heterogeneous catalytic reaction of gases: 2. A methanol conversion to olefins, J. Phys. Chem. 97 (1993) 3319–3323.

[37] Y. Yasuda, K. Iwai, K. Takakura, Novel rate constants for a catalytic hydrogenation reaction of propylene obtained by a frequency response method, J. Phys. Chem. 99 (1995) 17852–17861.

[38] Y. Yasuda, Y. Kuno, Novel kinetic model for heterogeneous catalysis based on free energy dissipation via intermediates deduced by the frequency response method, J. Phys. Chem. A 102 (1998) 4878–4882.

[39] Y. Yasuda, Y. Kuno, Free-energy dissipations via surface intermediates evaluated by the frequency response method in a catalytic hydrogenation of propene over rhodium, J. Phys. Chem. B 103 (1999) 3916–3922.

[40] M. Cavers, J.M. Davidson, I.R. Harness, G.S. MacDougall, L.V.C. Rees, Novel frequency response techniques for the study of kinetics in heterogeneous catalysis, Stud. Surf. Sci. Catal. 122 (1999) 65–72.

[41] A. Garayhi, F.J. Keil, Determination of kinetic expressions from the frequency response of a catalytic reactor — theoretical and experimental investigations, Chem. Eng. Sci., in press.

[42] F.J. Keil, Development of microkinetic expressions by instationary methods, submitted for publication.

[43] G. Marcelin, J.E. Lester, S.F. Mitchell, Frequency response study of the effect of alkali promotion on Rh/TiO$_2$ catalysts: evidence for kinetically distinct H$_2$-sorbing sites.

[44] Y. Yasuda, Frequency response method for investigation of gas/surface dynamic phenomena, Heterogen. Chem. Rev. 1 (1994) 103–124.

[45] M. Marwood, F. Van Vyve, R. Doepper, A. Renken, Periodic operation applied to the kinetic study of CO$_2$ methanation, Catal. Today 20 (1994) 437–448.

[46] R. Isermann, Identification of dynamic systems, Vol. 1, Springer, New York, 1992 (in German).

[47] V. Bourdin, Ph. Grenier, F. Neunier, L.M. Sun, Thermal frequency response method for the study of mass-transfer kinetics in adsorbents, AIChE J. 42 (1996) 700–712.

[48] J.J. DiStephano, A.R. Stubberud, I.J. Williams, Feedback and Control Systems, McGraw-Hill, New York, 1967.

[49] F.H.M. Dekker, A. Bliek, F. Kapteijn, J.A. Moulijn, Analysis of mass and heat transfer in transient experiments over heterogeneous catalysts, Chem. Eng. Sci. 50 (1995) 3573–3580.

[50] E.A. Mason, A.P. Malinauskas, Gas Transport in Porous Media: The Dusty-Gas-Model, Elsevier, Amsterdam, 1983.

[51] G.I. Golodets, Heterogeneous Catalytic Reactions Involving Molecular Oxygen, Vol. 15, Elsevier, Amsterdam, 1983, Stud. Surf. Sci. Catal.

[52] A. Mittasch, E. Theis, Von Davy und Döbereiner bis Deacon, ein halbes Jahrhundert Grenzflächenkatalyse, Verlag Chemie GmbH, Berlin, 1932.

[53] R.B. Anderson, K.C. Stein, J.J. Feenan, C.J.E. Hofer, Catalytic oxidation of methane, Ind. Eng. Chem. 53 (1961) 809–812.

[54] G. Kainz, H. Horwatitsch, The variable efficiency of metal and metal oxide catalysts in CH and N analysis, Microchim. Acta (1962) 7–15.

[55] J.G. Firth, H.B. Holland, Heterogeneous oxidation of methane over palladium catalysts, Nature 217 (1968) 1252–1253.

[56] J.G. Firth, H.B. Holland, Catalytic oxidation of methane on palladium–gold alloys, Trans. Faraday Soc. 62 (1966) 2566–2576.

[57] C. Kemball, Catalysis on evaporated metal films: II. The efficiency of different metals for the reaction between methane and deuterium, Proc. R. Soc. A 217 (1953) 376–389.

[58] R. Mezaki, C.C. Watson, Catalytic oxidation of methane, Ind. Eng. Chem., Proc. Des. Dev. 5 (1966) 62–65.

[59] A.P. Ahuja, G.P. Mathur, Application of initial rate technique for mechanism determination, Can. J. Chem. Eng. 45 (1967) 367–371.

[60] C.T. Campbell, D.C. Foyt, J.M. White, Partial oxidation of methane over heterogeneous catalyts, J. Phys. Chem. 81 (1977) 491–494.

[61] C.F. Cullis, D.E. Keene, D.L. Trimm, Oxygen penetration into the bulk of palladium, J. Catal. 19 (1970) 378–389.

[62] C.F. Cullis, B.M. Willatt, Oxidation of methane over supported precious metal catalysts, J. Catal. 83 (1983) 267–285.

[63] T.R. Baldwin, R. Burch, Catalytic combustion of methane over supported palladium catalysts: I. Alumina supported catalysts, Appl. Catal. 66 (1990) 337–358.

[64] M. Foka, J. Chaou Ki, C. Guy, P. Klvana, Natural gas combustion in a catalytic turbulent fluidized bed, Chem. Eng. Sci. 49 (1994) 4269–4276.

[65] R. Burch, F.J. Urbano, P.K. Loader, Methane combustion over palladium catalysts: the effect of carbon dioxide and water on activity, Appl. Catal. A 123 (1995) 173–184.

[66] P. Schneider, J.M. Smith, Adsorption rate constants from chromatography, AIChE J. 14 (1968) 762–771.

[67] P. Schneider, J.M. Smith, Chromatographic study of surface diffusion, AIChE J. 14 (1968) 886–895.